The Development of High Performance ITO Target. (Part II)

Kentaro UTSUMI
Yuichi NAGASAKI
Osamu MATSUNAGA
Akio KONDO

The ultra high density ITO target of 99[%] or more in relative density is developed by the improvements of ITO powder and the sintering process. EPMA analysis shows that the target has excellent uniformity of the distribution of Sn compared with the high density target prepared by the conventional process. The ultra high density target allows the resistivity of 150[$\mu\Omega\cdot$cm] or less, the high transmission of 83[%] or more in the optical region at the substrate temperature of 200[℃]. There are no nodules on the erosion racetrack of the ultra high density target at the end of its life.

Furthermore, the production process of the large size target and the long rectangle target is also developed by the improvements of the process.

1. INTRODUCTION

Thin film ITO (indium tin oxide) has been widely used as transparent conducting layers in various optoelectronic devices such as liquid crystal displays (LCDs), plasma displays and solar cells. The preparation processes of ITO thin film include spray[1], chemical vapor deposition (CVD)[2], evaporation[3-5] and sputtering. Among these methods, the most preferred method is reactive dc magnetron sputtering using ITO target because it is advantageous in its controllability of sputtering condition and adaptability to large area sputtering[6].

Recently, demands of higher density and larger size for ITO target has been increasing.

In this report, the results of developments of an ultra high density target and a large size target are described. Furthermore, effects of target density on sputtering and film characteristics are investigated.

2. ULTRA HIGH DENSITY TARGET

[1] DEVELOPMENT OF AN ULTRA HIGH DENSITY TARGET

(1) BACKGROUND

In continuous sputtering of the ITO target in an atmosphere of argon and oxygen gases, black nodules appear on the erosion racetrack of the target. Nodules are considered as a main cause of particles on substrates, and cleaning for target surface must be done frequently in production lines. This leads to reduction of producibility. The increase of target density is very effective to suppress the nodule formation[7], so that the higher density target is required.

Furthermore, a demand for low resistivity thin film is increasing. In the case of STN-LCD panels, with the increase of the panel size and higher resolution, significant problem of the increment of resistance of transparent electrode is occurred[8-9]. While, in the case of TFT-LCD panels, to reduce the production cost, a new ITO

process which is applied to forming source bus-lines of a large panel is developed[10]. This process also requires low resisitivity ITO thin film.

To reply these demands, we developed an ultra high density target.

(2) EXPERIMENTAL PROCEDURE

In of purity 99.99[%] and Sn of purity 99.99[%] were used as raw materials in this study. The size of ITO powder was optimized to obtain higher density. The ITO powder was then formed into a green body by the press method or the slip casting method.

In the case of the press method, the ITO powder was filled into desirable mold and pressed. At this time, binder such as polyvinyl alcohol or palaffin could be added.

While, in the case of the slip casting method, the ITO powder was mixed with de-ionized water, dispersant and binder to form slurry. The slurry was pored into a desirable mold. The green body was dried to remove water.

Then, both green bodies were cold isostatic pressed (CIPed). After the CIP treatment, the green bodies were dewaxed to remove dispersant and/or binder. Subsequently, the dewaxed green bodies were sintered at the atmospheric pressure. The sintering process was also optimized.

Target density was measured by Archimedes' method. The theoretical density of ITO was regarded as 7.156[g/cm^3].

Electron probe micro analysis (EPMA) and scanning electron microscopy (SEM) were used for analysis of the distribution of Sn and calculation of grain and pore size in the target.

(3) RESULTS

The relative density of the sintered bodies made by press method and slip casting method were 99.8[%]. Namely, the ultra high density targets (99[%] or more in relative density) were successfully sintered in production line.

Figure 1 shows the results of EPMA analysis for the ultra high density target (d=99.8[%]) and the high density target (d=97.8[%]) which was produced by conventional process : the SEM image (a) and the characteristic X-ray image of Sn-Lα (b) and In-Lα (c). It was observed that the distribution of Sn of the ultra high density target was more uniform than one of the high density target. The improvements of ITO powders were effective on the distribution of Sn.

The geometrical characteristics calculated with the SEM images of target surface are shown in Table 1. The pore size of the ultra high density target was about one-third of the high density target. It is clear that the increase of the sintered density corresponds to the decrease of the pore size.

〔2〕 EVALUATION OF THE ULTRA HIGH DENSITY TARGET

(1) EXPERIMENTAL PROCEDURE

The sputtering test was performed in a load-lock type dc magnetron sputtering system without arc killer. Three different sputtering targets 4inch×7inch×6[mmt] were used in this study. Table 2 shows the specifications of the targets.

Table 3 shows sputtering conditions. Discharge voltage, deposition rate, arcing frequency, particles stuck on the substrate, resistivity and transmittance were investigated. Arcing frequency was monitored as discharge current spikes which were converted into voltage pulses by a sensing coil inductively coupled with the

Table 1 Geometrical Characteristics Calculated with SEM Image

	Ultra High Density Target	High Density Target
Sintered Density	99.8[%]	97.8[%]
Grain Size	2.5[μm]	3.2[μm]
Pore Size	0.7[μm]	1.8[μm]

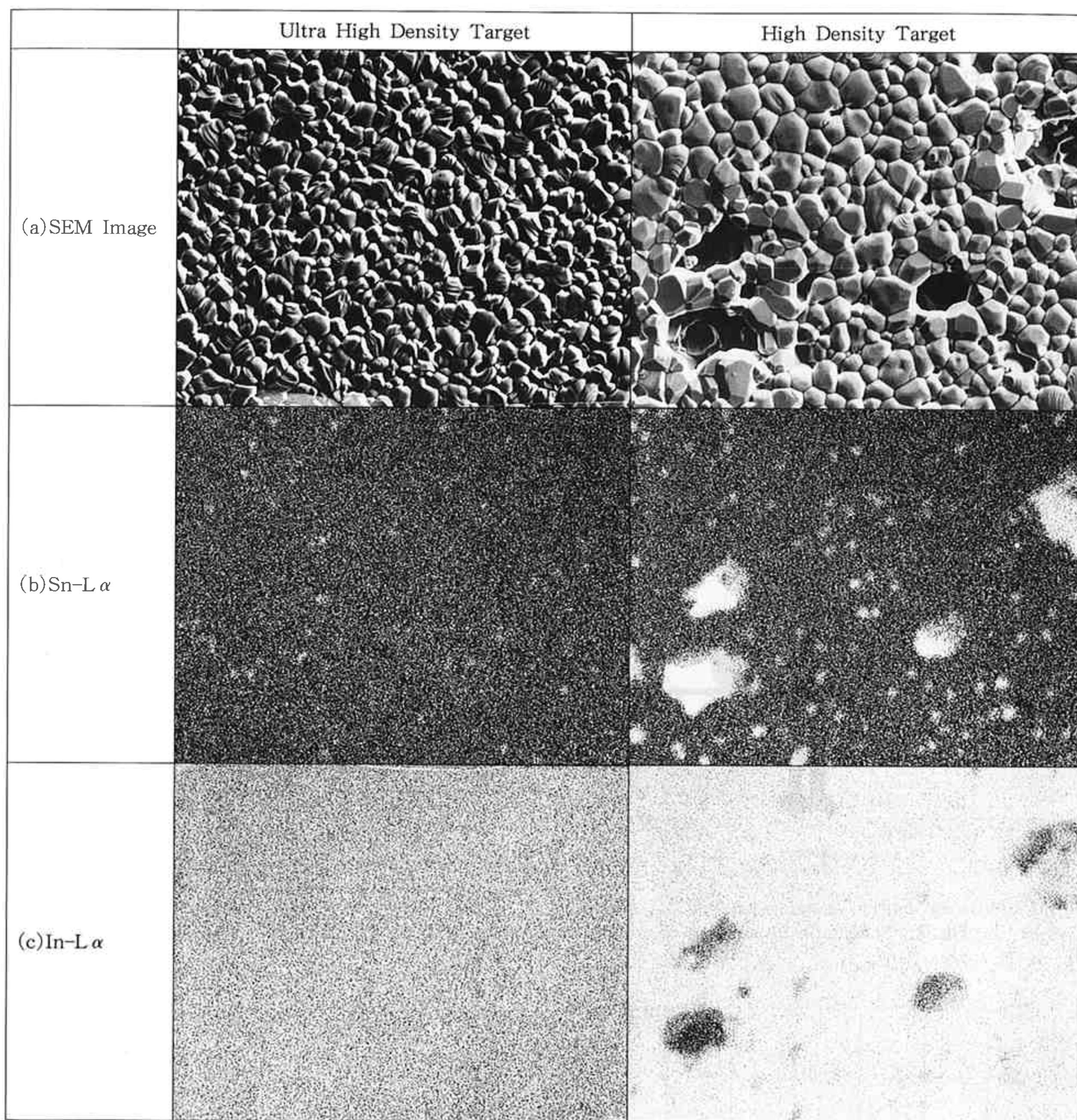

Fig. 1 Results of EPMA analysis for the ultra high density target and the high density target : the SEM image (a) and the characteristic X-ray image of Sn-L α (b) and In-L α (c).

Table 2 Specifications of ITO Target

Target Code	Density[%]	Production Process
A	99.0	Improved
B	96.8	Conventional
C	90.0	Conventional

Table 3 Sputtering Conditions

Substrate Temperature	200[℃]
Sputtering Pressure	5.0[mTorr]
DC Power Density	3.32[W/cm^2]
Sputtering Gas	Ar, Ar+5%O_2
Target Substrate Distance	10[cm]
Film Thickness	500[A]

power cable of the sputtering source (shown in Fig. 2). A laser particle counter and 4 inch semiconductor grade Si wafer were used for the measurements of particles.

For the ultra high density target, the continuous sputtering test was performed to investigate the nodule formation.

(2) RESULTS AND DISCUSSION

1) SPUTTERING CHARACTERISTICS

Figure 3 shows the dependence of discharge voltage on the target density. As the target density increased, the discharge voltage decreased. Generally, higher density targets have low resistance because of higher packing density by the decrease of the volume of pores. This is the main cause of the decrease of the discharge voltage of higher density target.

The dependence of deposition rate on the target density is shown in Fig. 4 . The deposition rate increased with the target density. In the case of the lower density target, because it has higher resistance, consumption of dc power at the target as the thermal energy increases. Therefore, substantial incident dc power decreases and the deposition rate decreases.

Figure 5 shows the dependence of arcing

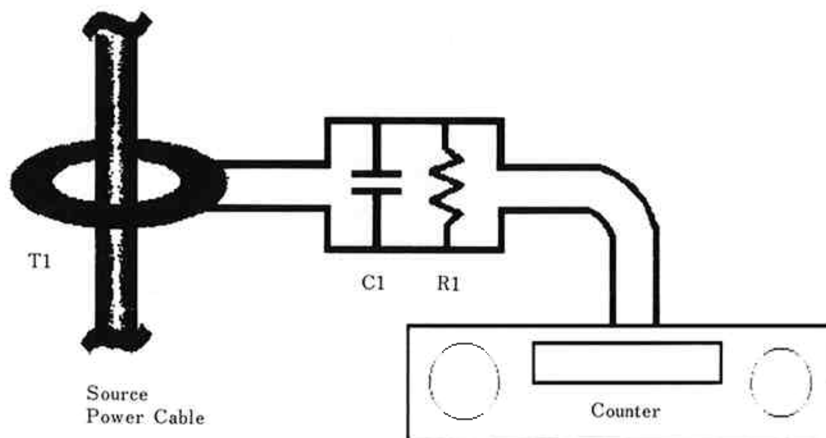

Fig. 2 Schematic illustration of arcing measurement. (By courtesy of C.E.Wickersham)

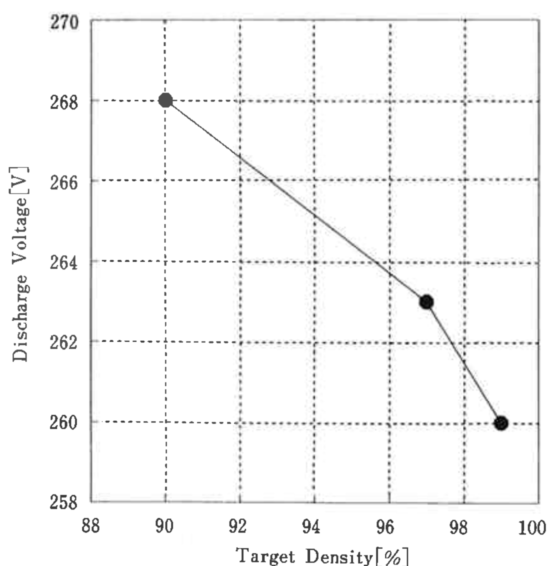

Fig. 3 The dependence of discharge voltage on the target density.

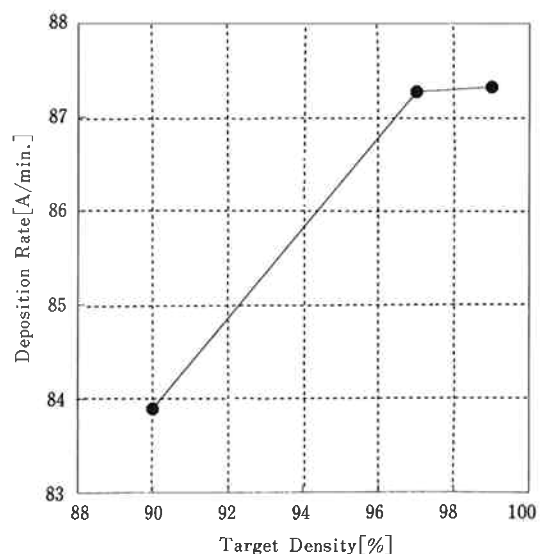

Fig. 4 The dependence of deposition rate on the target density.

frequency on the dc power for each target. The arcing frequency increased with the increase of dc power and the decrease of the target density. It is considered that one of reason of arcing occurrence is concentration of electrical field at the edge of pores of the target. The arcing occurs easily on lower density target with many pores.

Figure 6 shows the dependence of a number of particles on the target density. The number of particles decreased with the increase of the target density. It was reported by our previous study that the number of particles depended on the arcing frequency[11]. Therefore, the decrease of the number of particles is considered to be due to the decrease of the arcing frequency.

2) THIN FILM CHARACTERISTICS

The dependence of film resistivity on O_2/Ar is shown in Fig. 7. The minimum resistivity is obtained at 0.1[%] in O_2/Ar for each targets. Figure 8 shows the dependence of minimum resistivity on the target density. From 90[%] to

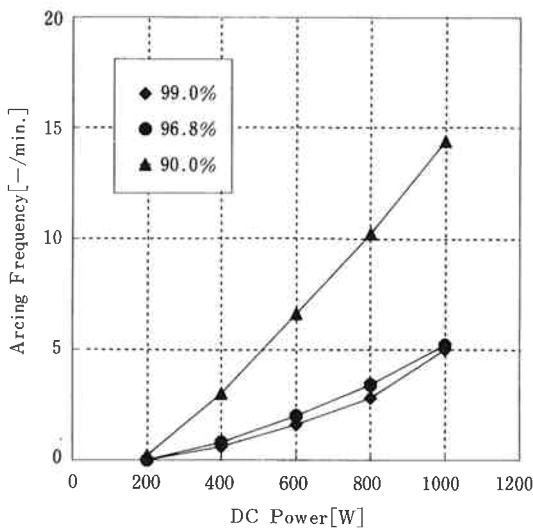

Fig. 5 The dependence of arcing frequency on the dc power.

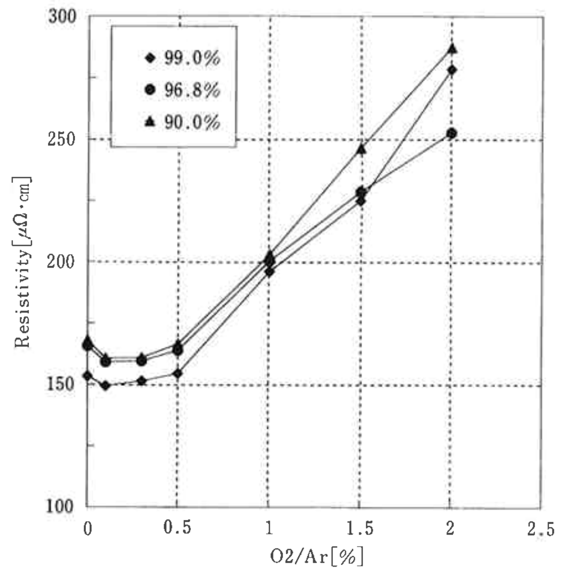

Fig. 7 The dependence of film resistivity on O_2/Ar.

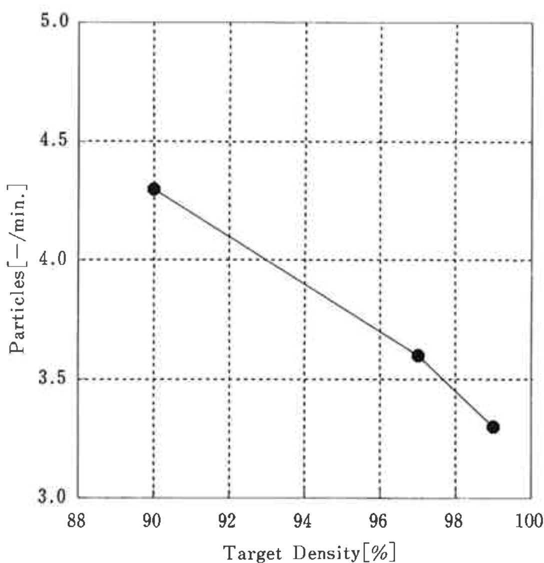

Fig. 6 The dependence of a number of particles stuck on the substrate on the target density.

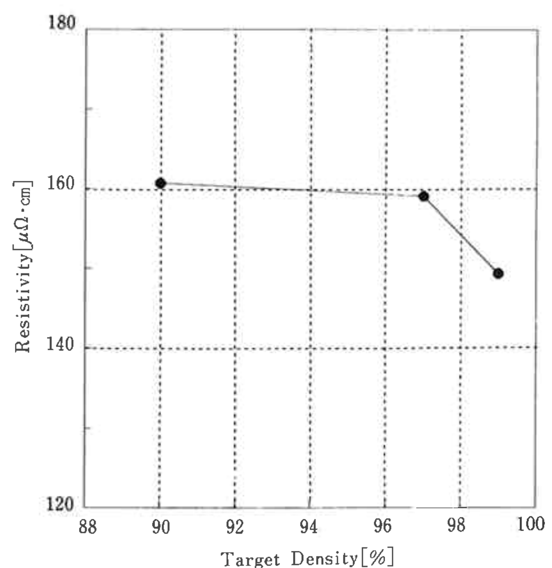

Fig. 8 The dependence of minimum resistivity on the target density.

97[%], resisitivity decreased slightly. From 97[%] to 99[%], however, it decreased rapidly. The targets of 90[%] and 97[%] are manufactured in the same conventional process. Therefore, the microstructure of the targets are almost the same except for the volume of pores.

It was reported that the resistivity decreased with the increment of the target density ranging from 70[%] to 90[%][12]. However, in this study, the improvement of resisitivity is not observed by the increment of the target density ranging from 90[%] to 97[%].

The ultra high density target of 99[%] is manufactured by the improved process, and its microstructure is different from the high density targets manufactured by the conventional process. Namely, the distribution of Sn of the ultra high density target is more uniform than one of the high density target. It is supposed that more uniform distribution of Sn in the target is effective on the thin film resistivity.

Figure 9 shows the dependence of the transmittance on wave length for each target. The transmittance of each thin film is almost the same. It was found that the target density and the distribution of Sn do not influence the transmittance.

3) CONTINUOUS SPUTTERING TEST

Figure10 shows the optical photograph of the surface of the ultra high density target at the end of its life. It was found that there are no nodules on the erosion racetrack of the target. It was reported that nodules were generated as the remainder of sputtering due to high resistivity and low sputtering yield substances which were introduced by arcing at the edge of pores[11]. By the development of the ultra high density target having the fewer pores, the nodule-less ITO target is obtained.

3 . LARGE SIZE TARGET

Recently, mother glass for LCD has been changing from the second generation (360×465 ～400×500[mm]) to the third generation (550×650[mm]) in the production line. Furthermore, a new efficient sputtering system, namely a cluster type sputtering system has been introduced into the TFT-LCD production lines. Therefore, the large size target for the cluster type sputtering system and the long rectangle size target for the in-line sputtering system have been required.

In the case of the cluster type sputtering system, the target size is 550×640～565×690[mm] for the second generation substrate, and 800×800[mm] or more for the third generation substrate. While, in the case of the in-line system, a long axis of the target is 700[mm] for the second generation substrate, and 900[mm] or more for the third generation.

Moreover, it is required that the target will be made of single tile because of prevention of particle generation in the gap of the tiles during

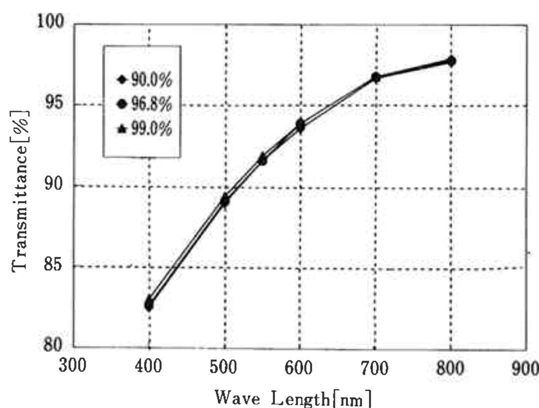

Fig. 9 The dependence of the transmittance on wave length.

Fig. 10 The optical photograph of the surface of the ultra high density target at the end of its life.

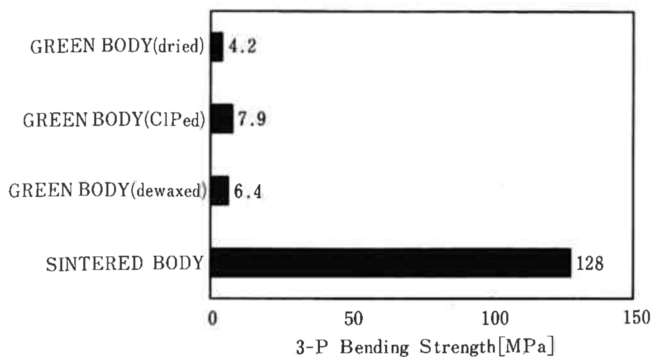

Fig.11　Bending strength at each stage.

sputtering.

The most significant problem in this development was fragility of the green body. The bending strength of the green body is about 4.2～7.9[MPa], while the one of the sintered body is 128[Mpa] (shown in Fig.11). As the size of the target is larger, the green body is broken more easily. The further addition of binder makes the green body strong. However, that degrades the properties of the sintered body. Therefore, the improvements of the process to prevent break were carried out.

Furthermore, the machining of ceramic materials such as ITO is more difficult than metallic materials because the ceramics have more brittleness. For that reason, the sintered body is formed with the near net shape.

Consequently, the single tile ITO target for the second generation substrate was developed (shown in Fig.12).

And also, the target with three tiles for the third generation one was developed.

4. CONCLUSIONS

The ultra high density ITO target of 99[%] or more in relative density which has excellent uniformity of the distribution of Sn has been developed by the improvements of the ITO powders and the sintering process. By using the target, the resistivity of 150[$\mu\Omega\cdot$cm] or less is obtained at the substrate temperature of 200[℃]. There are no nodules on the erosion racetrack of the ultra high density target at the end of its life.

The production process of the large size target

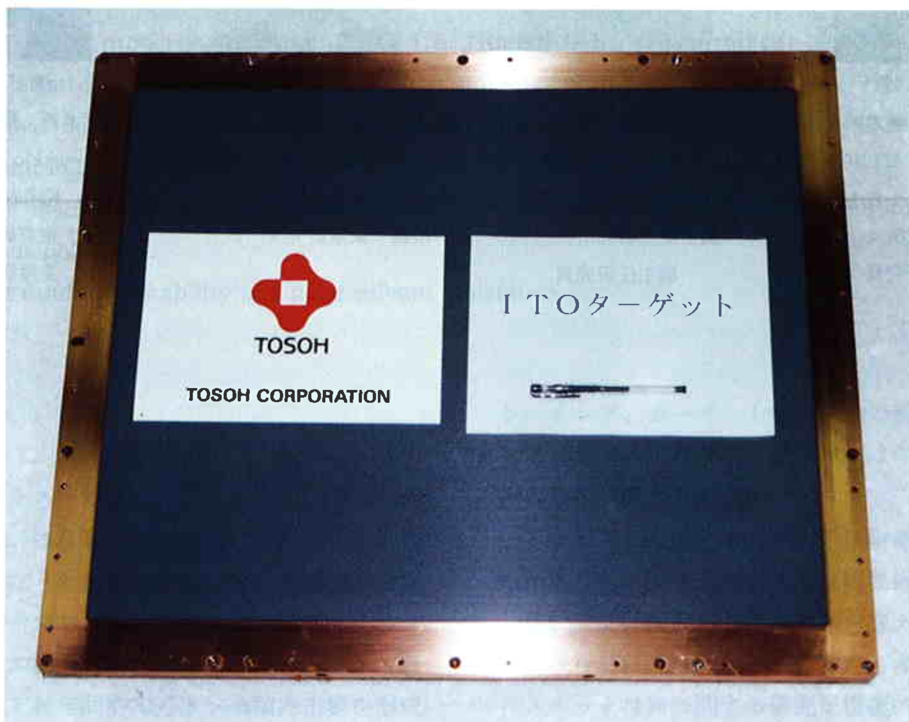

Fig.12　The optical photograph of the single tile ITO target for the second-generation substrates.

and the long rectangle target have been also developed. The single tile ITO target for the second generation substrate and the target with three tiles for the third generation one have been advanced to the commercially available stage.

5. ACKNOWLEDGMENTS

The authors would like to thank Dr. C. E. Wickersham at TOSHO SMD Inc. for useful discussion of this work and suggestion of the arcing measurements.

References

1) A. K. Saxena, S. P. Singh, R. Thangaraj and O. P. Agnihotri, Thin Solid Films, 117, 95 (1984).
2) T. Maruyama and K. Fukui, Thin Solid Films, 203, 297 (1991).
3) I. Hamberg and C. G. Granqvist, J. Appl. Phys., 60, 11 (1986).
4) Y. Shigesato and I. Yasui, Sputtering & Plasma Processes, 11, 1, 39 (1996).
5) S. Wada, M. Koyama, H. Saito, T. Sakemi, M. Tanaka and K. Awai, Sputtering & Plasma Processes, 11, 1, 49 (1996).
6) R. Latz, K. Michael and M. Scherer, Jpn. J. Appl. Phys., 2, 30 (2A), 149 (1991).
7) K. Utsumi, T. Takahara, Y. Suzuki and A. Kondo, J. TOSOH Res., 38, 33 (1994).
8) M. Higuchi, Jpn. MRS Symposium, L11, 125 (1996).
9) H. Saito, Fineprocess Technology Jap. '96 Confernce Proceedings, R-9, 10 (1996).
10) M. Katayama, Jpn. MRS Symposium, L12, 125 (1996).
11) K. Utsumi and A. Kondo, Jpn. MRS Symposium, LP2, 128 (1996).
12) R. Yoshimura, N. Ogawa and T. Mouri, J. TOSOH Res., 36, 153 (1992).
13) C. E. Wickersham, Private Communication.

著　者
氏名　内 海　健太郎
Kentaro UTSUMI
入社　昭和61年4月1日
所属　東京研究所
副主任研究員

著　者
氏名　長 崎　裕 一
Yuichi NAGASAKI
入社　昭和62年4月1日
所属　東京研究所
副主任研究員

著　者
氏名　松 永　修
Osamu MATSUNAGA
入社　平成4年4月1日
所属　東京研究所

著　者
氏名　近 藤 昭 夫
Akio KONDO
入社　昭和51年4月16日
所属　東京研究所
主席研究員